0026-895X/90/020164-09$02.00/0

MOLECULAR PHARMACOLOGY, 37:164-172

A Natural Processing Product of Rat Diazepam Binding Inhibitor, Triakontatetraneuropeptide (Diazepam Binding Inhibitor 17–50) Contains an α-Helix, Which Allows Discrimination between Benzodiazepine Binding Site Subtypes

ALLA BERKOVICH, PETER MCPHIE, MARIE CAMPAGNONE, ALESSANDRO GUIDOTTI, and PRESTON HENSLEY

Fidia-Georgetown Institute for the Neurosciences, Washington, DC 20007 (A.B., M.C., A.G.), National Institute of Diabetes and Diseases of the Kidney, National Institute of Health, Bethesda, Maryland 20205 (P.M.), and Macromolecular Science Department, Smith Kline and French Research and Development Laboratories, King of Prussia, PA 19406-0939 (P.H.)

Received March 30, 1989; Accepted October 16, 1989

SUMMARY

Synthetic peptides related to triakontatetraneuropeptide (TTN) [^{17}TQPTDEEMLFIYSHFKQATVGDVNTDRPGLLDLK^{50}; diazepam binding inhibitor (DBI) 17–50], a natural brain processing product of rat DBI, were analyzed for their physicochemical and ligand-receptor interaction characteristics. The ability of TTN and TTN-related fragments to displace [^{3}H]flumazenil (ethyl-8-fluoro-5,6-dihydro-5-methyl-6-oxo-4*H*-imidazo[1,5a][1,4]-benzodiazepine-3-carboxylate) or [^{3}H]Ro 5-4864 [7-chloro-1,3-dihydro-1-methyl-5-(*p*-chlorophenyl)-2*H*-1,4-benzodiazepine-2-one] from their respective benzodiazepine (BZ) binding site subtypes was tested in intact cerebellar culture neurons or in homogenates of cultured astrocytes. These studies indicate that the C-terminal region of TTN, which is also present in DBI 22–50, eicosapentaneuropeptide (DBI 26–50), and octadecaneuropeptide (ODN) (DBI 33–50), but not in DBI 19–41, is essential for interaction with the BZ recognition sites. When the C-terminal lysine of ODN is blocked with an NH_2 group, the ability of ODN to interact with the binding of [^{3}H]flumazenil is lost. A comparison analysis of the binding data with the secondary structure characteristics of the peptides demonstrated that TTN (DBI 17–50) and DBI 22–50, which have hydrophobic portions and marked tendencies to produce α-helicity, specifically displace (apparent K_i, 5–6 μM) [^{3}H] Ro 5-4864 from astroglial cell binding sites. Peptides (ODN, eicosapentaneuropeptide, OND-NH_2) with very low tendencies to form α-helices and with virtually no hydrophobic structure were not able to displace Ro 5-4864 at concentrations of up to 100 μM. In contrast, ODN was a good displacer of [^{3}H]flumazenil from intact neurons, with an apparent IC_{50} of 5 μM. These data suggest that the α-helical portion of TTN may be important for BZ receptor recognition and BZ receptor subtype discrimination.

A newly discovered family of neuropeptides derived from a common neuropeptide precursor, DBI, and acting as negative allosteric modulators of $GABA_A$ receptors at various BZ recognition sites (1, 2), were analyzed for their physicochemical and ligand-receptor interaction characteristics. DBI is a M_r 10,000 polypeptide found in high concentrations in brain and specific peripheral tissues of several mammalian species (3–5).

DBI can be cleaved posttranslationally into biologically active fragments by the action of brain-specific endopeptidases (1, 2). Recently, three major endogenous neuropeptides with primary structure derived from region 17–50 of DBI, all containing the amino acid sequence structure of DBI 33–50 at the C-terminal region, were found in rat brain (2, 6). These neuropeptides are TTN (DBI 17–50) which is the most abundant, EPN (DBI 26–50), and ODN (DBI 33–50). They appear to produce similar pharmacological activities (for example, they induce conflict behavior when injected into rats), but they have different intrinsic sites of action at different subtypes of BZ recognition sites. TTN is virtually devoid of action on the binding of the anxiolytic BZs, but it displaces the anxiogenic and convulsant BZ Ro 5-4864 from its specific binding sites, either those linked to mitochondrial membranes or those associated with a specific $GABA_A$ receptor subtype (1, 2).

In contrast ODN and EPN displace [^{3}H]flunitrazepam or [^{3}H]flumazenil more potently and efficiently than they displace [^{3}H]Ro 5-4864 from their respective BZ binding sites in neuronal membranes (1, 2, 6). The proconflict action of TTN in rats is blocked by the isoquinoline carboxamide PK 11195, an antagonist of Ro 5-4864 (1, 2); the proconflict action of ODN and EPN, however, is not blocked by PK 11195 but is blocked by flumazenil, an antagonist of BZ and β-carboline ester action at the $GABA_A$ receptors (1, 2, 6). The different mechanisms whereby TTN, EPN, and ODN express an apparently similar pharmacological profile led us to analyze in detail the primary

ABBREVIATIONS: DBI, diazepam binding inhibitor; TTN, triakontatetraneuropeptide; EPN, eicosapentaneuropeptide; ODN, octadecaneuropeptide; BZ, benzodiazepine; BOC, *N-tert*-butoxycarbonyl; HPLC, high pressure liquid chromatography; MeOH, methanol; SDS, sodium dodecyl sulfate.

structural requirement of the C- and N-terminal region of these peptides for the expression of biological activity. Moreover, in order to interpret in structural terms the ability of TTN, ODN, and EPN to discriminate among the different BZ recognition site subtypes, we have also considered the secondary structural characteristics of these peptides.

Materials and Methods

Peptide synthesis. The peptides were synthesized by the Merrifield solid-phase technique (7) with a Beckman 990 automated synthesizer. Amino acids were coupled to a chloromethylated polysterene divinylbenzene resin (Peninsula Laboratories, San Carlos, CA). All Boc-amino acids were of the L-configuaration and were purchased from Bachem (Torrance, CA). Boc-Met and Boc-Glu (γ-benzyl ester) were purchased from Peninsula; Boc-His was used with *N*-π-benzyloxymethyl protection. Asparagine and glutamine were incorporated into the peptide with an unprotected side chain in the presence of 1 equivalent of 1-hydroxybenzotriazole. Diisopropylcarboiimide (Aldrich Chemical Co, Milwaukee, WI) was used as the coupling agent. Coupling was performed with a 6-fold excess of Boc-amino acids and monitored by the ninhydrin test (8). The protected peptide-resin was dried under vacuum and treated with the low and high HF procedure at 0° (9). After removal of the HF under N_2, the resin was washed with ethyl ether (Fisher Chemicals, Fair Lawn, NJ). The peptide was extracted from the resin with 15% and/or 50% acetic acid.

Peptides were purified by gel filtration on Sephadex G-10 (Pharmacia, Piscataway, NJ), with final purification by HPLC with a 7.8 mm × 30 cm semipreparative reverse phase C_{18} μ-Bondapak column (Waters, Milford, MA). The synthetic material was eluted with a 2-hr gradient from 10% to 60% H_2O/acetonitrile containing 0.1% trifluoroacetic acid.

Purity of the peptides was confirmed by thin layer chromatography using 1-butanol, 4/acetic acid, 1/H_2O, 1, and 1-butanol, 15/acetic, 3/water, 12/pyridine, 10, by reverse phase HPLC, and by amino acid analysis. Amino acid composition was determined in samples of peptides hydrolyzed in 6 N HCl at 110° for 24 hr, by conventional ion exchange technique using a Beckman 6000 amino acid analyzer. Amino acid sequence analysis was performed with a gas phase sequinator and the amino acids were detected by HPLC using phenylthiohydantoin derivatization (10). β-Endorphin (human 1–27) was purchased from (Bachem).

Hydrophobicity analysis. In order to determine the conformational characteristics of DBI, an analysis of the secondary structure was performed by the method of Chou and Fasman (11).[1] We used an algorithm described by Rose *et al.* (12), which determined the hydrophobicity according to the scales of Kyte and Doolittle (13), Nozaki and Tanford (14), and Hopp and Woods (15).

CD spectra. CD spectra of the peptides (10–20 μM) were obtained in H_2O, SDS, and MeOH solution at 4° and 25°. Care was taken that the absorbance of each peptide solution never exceeded 1.0. The spectropolarimeter was calibrated between 290 and 195 nm with D-camphor sulphonic acid. CD spectra were recorded between 200 and 260 nm, using a Jasco J-500 C spectropolarimeter equipped with a DP-500N data processor. Spectra were recorded digitally and analyzed in terms of secondary structure using the CONTIN program (16). The measured rotations were converted into mean residue ellipticity [θ], using the equation:

$$\theta = \frac{\text{Rotation (m°)} \times 10 \times \text{mean residual weight}}{\text{Path (cm)} \times \text{conc (mg/ml)} \times 100}$$

Binding studies. The displacement of [^{3}H]flumazenil or [^{3}H]Ro 5-4864, respectively, bound to intact cerebellar granule cells or to homogenates of cerebellar astrocytes was used to evaluate the binding of the various processing products of DBI. Primary cultures of cerebellar granule cells were prepared from 8-day-old rats (17) and were characterized as described by Vaccarino *et al.* (18). Binding studies were carried out on cultures plated on 35-mm dishes. The dishes were washed twice with 2 ml of Locke's solution (6) and then incubated with 1 ml of Locke's solution at 4° for 60 min, in the presence of 2 nM [^{3}H] flumazenil with or without the peptide to be tested. The assay was stopped by washing the cells rapidly three times and by resuspending them in 1 ml of 0.1 N NaOH. A 0.1-ml aliquot of this suspension was used for protein determination (19). Nonspecific binding was taken as the radiolabeled ligand bound to cells in the presence of 2 μM diazepam.

Primary cerebellar astrocytes grown to confluency in 75-ml flasks (20) were harvested and washed twice with 0.9% saline. The cells were homogenized with a Polytron (setting 6) for 15 sec in cold (4°) 50 mM Tris acetate, pH 7.4. After centrifugation at 48,000 × *g* for 20 min, the resultant pellet was resuspended in 50 mM Tris acetate, pH 7.4, to obtain a protein concentration between 0.2 and 0.3 mg/ml. Binding was performed in a final volume of 250 μl containing 200 μl of cell homogenate, 2 nM [^{3}H]Ro 5-4864, and various concentrations of the peptides under study. After incubation at 4° for 60 min, the binding reaction was stopped by addition of 2 ml of ice-cold Tris buffer, followed by rapid filtration over glass fiber Whatman GF/C filters. Nonspecific binding was obtained by incubation with 10 μM diazepam or Ro 5-4864.

The specific binding of [^{3}H]flumazenil or [^{3}H]RO 5-4864 to neurons or glial cells, respectively, was saturable, and the dissociation constants (K_d) and the maximal number of binding sites (B_{max}) were derived by a Scatchard analysis of the primary binding data. IC_{50} values were calculated from competition studies using 8–10 data points.

The binding assay for [^{3}H]dihydroalprenolol was carried out for 60 min at 4° on glial cell homogenates in Tris buffer (see above), using different concentrations of [^{3}H]dihydroalprenolol (1–10 nM). The specific binding was determined as the difference between total binding and binding in the presence of 10 μM (−)-alprenolol.

Results

Hydrophobicity of DBI. Fig. 1 shows the hydrophobicity profiles of DBI determined by the method of Hopp and Woods (15), Kite and Doolittle (13), and Nozaki and Tanford (14). By all three methods, rat DBI has a major hydrophobic region located between amino acid residues 31 and 35 and centered at amino acid residue 28.

Secondary structural analysis. The secondary structure of rat DBI was predicted by the method of Chou and Fasman (11). The results of the analysis are also given in Fig. 1, together with the charge distribution. This analysis predicts that in DBI there are three α-helical regions. The first region extends from amino acid residues 8 to 17, the second from residues 23 to 37, and the third from residues 67 to 81. The rest of the DBI structure is dominated by β-turn segments; there appears to be no significant β-sheet structure. Interestingly, the second predicted α-helix superimposes exactly on the region of the peptide that displays maximal hydrophobicity. This region is included in the structure of TTN. To better visualize this helix, a helical wheel diagram of DBI, from residues 23 to 37, is shown in Fig. 2. From this diagram it is evident that the hydrophobic residues (11 of 15 amino acids) are distributed more or less randomly around the helix and, hence, the helix does not have an obvious amphipathic nature. The N-terminal region of the helix is characterized by three negatively charged amino acids (Asp_{21}, Glu_{22}, and Glu_{23}) separated from two positive amino acids (i.e., His_{30} and Lys_{32}) by six uncharged amino acids.

CD spectra of DBI peptide fragments. To determine whether the predicted α-helix (residues 23–37) can form in solution, CD spectra of synthetic DBI peptide fragments, in-

[1] Thanks to M. Karrels (University of California, Berkeley) for providing us with the algorithm.

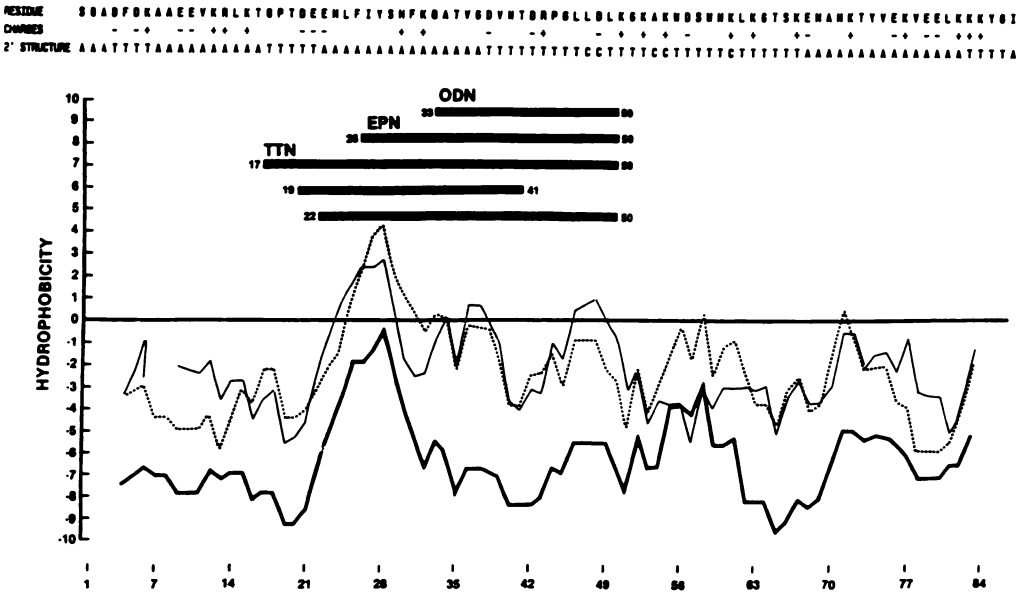

Fig. 1. Physicochemical characteristics of rat DBI. (a) The *top line* of the figure contains the amino acid sequence of rat DBI and its fragments expressed according to one letter notation; (b) the *second line* gives the amino acid charges; (c) the *third line* is the predicted secondary structure determined by the method of Chou and Fasman (11); (d) the *bottom portion* of the figure shows the hydrophobicity profiles of DBI predicted by the methods of Hoop and Woods (15) (· · · ·), Kyte and Doolittle (13) (——), and Nozaki and Tanford (14) (——), respectively.

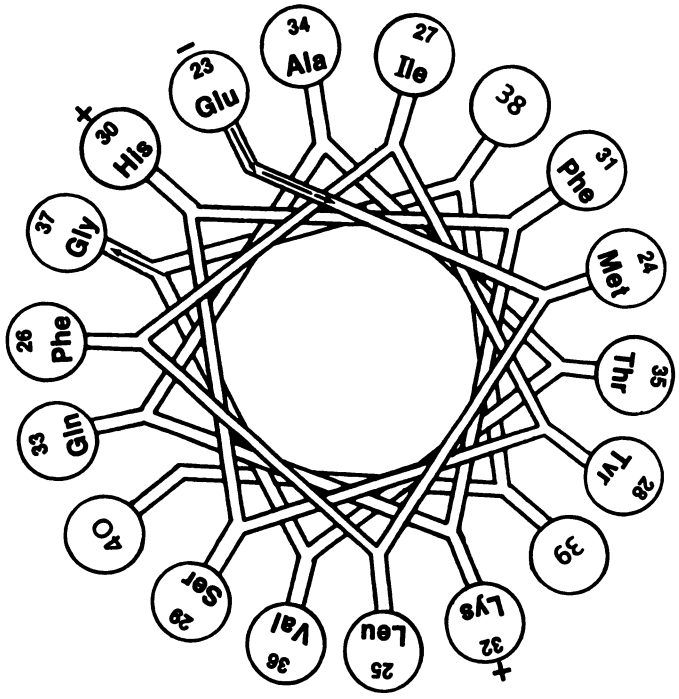

Fig. 2. Helical wheel diagram of DBI (23–37).

cluding TTN (DBI 17–50) and four related shorter peptides (DBI 22–50, DBI 26–50, DBI 19–41, and DBI 33–50; see Fig. 1), were analyzed in three solvent conditions at 4° (the same temperature at which the binding assay was conducted). Fig. 3 shows CD spectra of the synthetic peptides in H_2O (upper spectrum in each panel), 0.1% SDS (middle spectrum in each panel), and 100% MeOH (lower spectrum in each panel). In H_2O, all peptides studied yielded minimal ellipticity and none of the peptides showed the clear presence of double minima, suggesting lack of probability for forming α-helical structures under this solvent condition. In contrast, in SDS and even more pronounced in MeOH, some peptides (TTN, DBI 22–50, and DBI 19–41) produced pronounced spectral rotation and double minima between 210 and 220 nm, suggesting that they yielded significant α-helical structure (Fig. 3). Absence of apparent double minima at 210–220 nm in the spectra of ODN and EPN in SDS or MeOH (Fig. 3) suggests that these two peptides are virtually incapable of producing an α-helical structure (Fig. 3, D and E). From the data of Fig. 3, the predicted amount of α-helix and β-sheet was determined, applying the computer analysis technique previously used for the determination of the secondary structure of globular proteins (16). There are clear limitations in applying these analyses to small nonglobular peptides; however, we have observed good agreement between the values obtained with these calculations and the number of amino acids in the helix as predicted by the method of Chou and Fasman (11). For TTN in MeOH (a condition of low dielectric constant that mimics a hydrophobic environment), the spectrum suggests 48% α-helix and 19% β-sheet probability (Table 1). In terms of amino acid residues, this analysis predicts that 16.3 residues should be α-helical. This is in good agreement with the 15-amino acid helix suggested by the prediction method of Chou and Fasman (Fig. 1). The CD spectra of four other DBI fragments are given in Fig. 3, B–E. A similar analysis of their secondary structure is given in Table 1. CD spectra of peptide 22–50 suggests 28% α-helix, with the prediction of eight amino acids in the α-helix. Peptide 19–41, which contains the predicted α-helical part of TTN, has a helical profile in MeOH which suggests 23% α-helicity and predicts a number of amino acids (5.3) in the α-helix. Spectra of EPN and ODN (Fig. 3, D and E) showed no tendency to helicity, as well as a lack of double minima between 210 and 220 nm (α-helical prediction around 10%), and suggest a small number of α-helical amino acids (approximately two amino acids each) (Table 1).

In another group of experiments the spectra of the synthetic DBI fragments were analyzed at 22°. Although the trend to form an α-helical structure was similar to that at 4°, the predicted helicity was less pronounced than at 4° (data not shown) and the results were more difficult to interpret in quantitative terms because the peptide-induced spectra rotations were closer to noise values.

Binding studies. The inhibition by the different synthetic

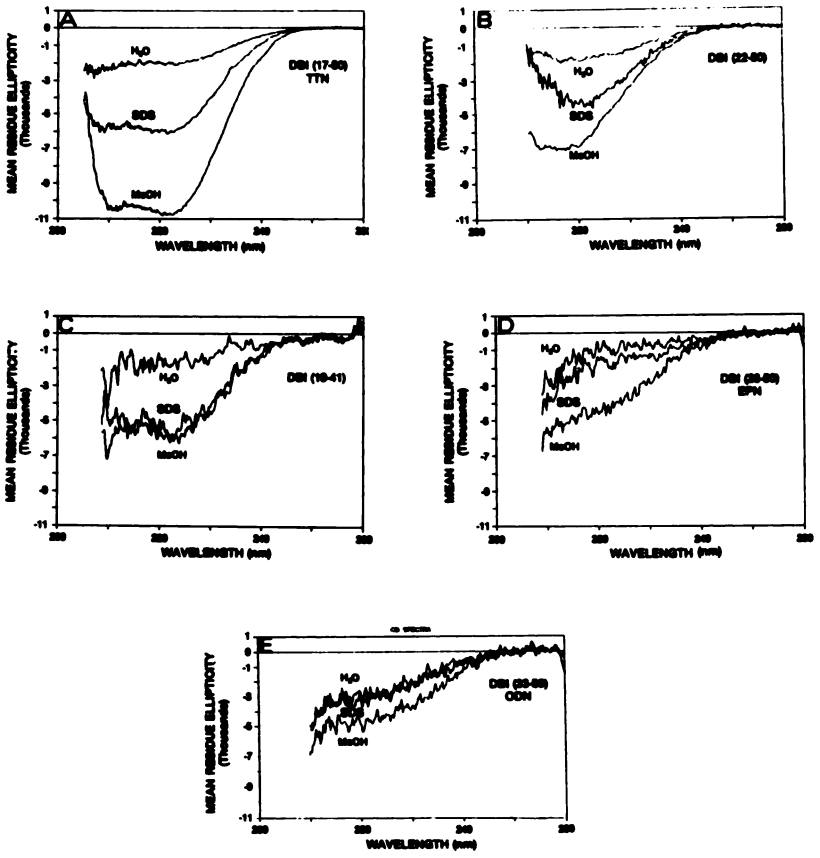

Fig. 3. A, CD spectra of DBI (17–50); B, DBI (22–50); C, DBI (19–41); D, DBI (26–50); E, DBI (33–50) in the far UV region. The spectra of 10–20 μM peptide were determined at 4° in H_2O (*upper spectrum* in each *panel*), 0.1% SDS (*middle spectrum*), and 100% MeOH solution (*lower spectrum*).

TABLE 1

Secondary structure of DBI 17–50 and its fragments at 4°

These data (mean value of three analyses with 5–10% variation) are derived from the CD spectra of Fig. 3 using the method of Provencher and Glockner (16). An analysis at 22° reveals similar secondary structure characteristics; however, the spectra rotation show lower ellipticity, making a quantative evaluation more difficult.

Peptide	Solvent	Helix	Sheet	Amino acids in helix
		%	%	
TTN (DBI 17–50)	Water	9	46	3.1
	SDS	22	37	7.5
	MeOH	48	19	16.3
DBI 22–50	Water	0	46	0
	SDS	11	45	3
	MeOH	28	34	7.8
EPN (DBI 26–50)	Water	0	46	0
	SDS	4	46	1
	MeOH	8[a]	55	2.2
ODN (DBI 33–50)	Water	3	42	0.5
	SDS	2	46	0.5
	MeOH	7[a]	41	2.0
DBI 19–41	Water	0	44	0
	SDS	20	33	4.6
	MeOH	23	34	5.3

[a] The CD spectra of EPN and ODN (see Fig. 3) do not show clear α-helical structure and the calculated numbers represent threshold values for α-helical probability.

peptides of the binding of Ro 5-4864 [a ligand for the $GABA_{A3}$ or mitochondrial-linked BZ binding sites (21)] to crude membranes prepared from neonatal rat cerebellar astrocytes in primary culture or of the binding of [^{3}H]flumazenil [a specific ligand for BZ binding sites located on the allosteric center of $GABA_{A1}$ or $GABA_{A2}$ receptors (21)] to primary culture of cerebellar granule cells was evaluated in order to correlate the predicted physicochemical characteristics of the peptides with their biological activity toward different BZ recognition site subtypes. [^{3}H]Flumazenil binds to intact neurons with an apparent K_d of 10 nM and a B_{max} of 0.5 pmol/mg of protein. [^{3}H] Ro 5-4864 binds to astrocyte membranes with an apparent K_d of 10 nM and a B_{max} of 25 pmol/mg of protein. Fig. 4 shows a typical displacement curve of [^{3}H]Ro 5-4864 binding by different fragments of DBI. TTN (DBI 17–50) and DBI 22–50, which

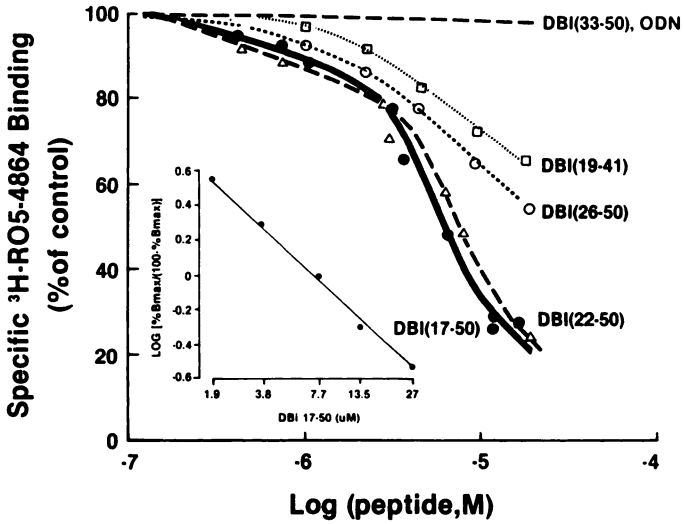

Fig. 4. Inhibition of [^{3}H]Ro 5-4864 binding to membrane of rat astrocytes by synthetic fragments of DBI. Each *point* represents the mean of five assays conducted in a typical experiment. Similar results were obtained in five or six different experiments. The variation in each experiment was less than 10% of the mean. *Inset*, the Hill plot of the TTN (DBI 17–50) data.

contain the full predicated α-helix (see Fig. 3 and Table 1), are the most potent in displacing [^{3}H]Ro 5-4864 binding. For both TTN and DBI 22–50, the Hill coefficient approaches unity (see Fig. 4, *inset*), suggesting that the peptide binds to a population of noninteracting binding sites. The apparent K_i values for TTN and DBI 22–50 for [^{3}H]Ro 5-4864 recognition sites were determined to be 5 and 6 μM, respectively. Table 2 shows that TTN (DBI 17–50) and DBI 22–50 are unable to displace [^{3}H] flumazenil from cultured neurons in concentrations up to 100 μM. In contrast, ODN (DBI 33–50), which includes no helix (see Fig. 3) and does not possess the lipophilic structure of TTN (see Fig. 1), displaces [^{3}H]flumazenil from cultured neurons with an apparent K_i of 5 μM but is virtually unable to displace [^{3}H]Ro 5-4864 from astroglial homogenates (Table 2). Interestingly, amidation of the carboxyl terminal lysine of ODN to form ODN-NH_2 abolishes the ability of ODN to displace [^{3}H]flumazenil (Table 2).

DBI 26–50, which has low predicted helicity and lacks negative charges on the amino terminus, and DBI 19–41, which has a full α-helix with the hydrophobic part of TTN but does not contain the carboxyl terminal part of ODN, displaces [^{3}H] Ro 5-4864 with a IC_{50} higher than 50 μM (see Fig. 4). For both DBI 26–50 and DBI 19–41, the Hill coefficient number is less than 1 (approximately 0.5), suggesting noncompetitivity. In experiments not reported here, [^{3}H]flunitrazepam (2 nM), [^{3}H] β-carboline-3-carboxylate methyl ester (2 nM), and [^{3}H]diazepam (10 nM) were also used as ligands to study the effect of peptides on the BZ binding sites in intact cerebellar neurons and glial cell homogenates. The results obtained with these ligands confirmed previous reports (2, 6, 22, 23) and were similar to those obtained in Fig. 4 and Table 2, using [^{3}H] flumazenil. However flunitrazepam, [^{3}H]β-carboline-3-carboxylate methyl ester, and diazepam are ligands susceptible to the "GABA shift" (24), whereas [^{3}H]flumazenil is not. Therefore, [^{3}H]flumazenil was used for routine analyses.

Ro 5-4864 binding sites can also be recognized by PK 11195. In a group of experiments, the effect of TTN and its related peptides on the binding of [^{3}H]PK 11195 to astrocytic membranes was studied. TTN and its analogues displace [^{3}H]PK 11195 from its binding sites with a potency and efficiency similar to that reported for [^{3}H]Ro 5-4864 (data not shown).

To exclude that the effect of TTN on [^{3}H]Ro 5-4864 binding was the consequence of a nonspecific interaction between the α-helical structure of the peptide and Ro 5-4864 we compared the effect of TTN with that of β-endorphin (a peptide of 31 amino acids that also possesses a stable α-helical structure; see Ref. 25). As shown in Table 3, β-endorphin failed to inhibit [^{3}H]Ro 5-4864 binding. Table 3 also shows that TTN, in a dose that strongly inhibited [^{3}H]Ro 5-4864 binding, failed to inhibit [^{3}H]dihydroalprenolol binding.

To further exclude that the effect of TTN on [^{3}H]Ro 5-4864 binding was the consequence of a physicochemical interaction between the peptide and the radioligand, we incubated for 60 min, at 4°, 2 nM [^{3}H]Ro 5-4864 with 10 μM TTN in 50 μM Tris acetate buffer, pH 7.4. At the end of the incubation period, TTN was rapidly (30 sec) separated from the free radioactive ligand by the centrifugation method of Penefsky (26), using a Sephadex G10 column as described by Massotti *et al.* (27). No radioactivity was bound to TTN under these conditions.

Discussion

Structural considerations. The α-helical portions of the peptide ligands appear to be important for receptor recognition and receptor subtype discrimination (25, 28). Hence, the secondary structure of DBI and of DBI specific peptide fragments was predicted to see whether similar principles were operating with respect to the binding of DBI (or its fragments) to specific BZ binding site subtypes. The secondary structural prediction of Fig. 1 suggests that the naturally occurring ligand TTN (DBI 17–50) (2) contains an α-helix (residues 23–37), a region predicted to be β-turn (residues 17–22) located on the N-terminus, and a predicted β-turn segment located in the C-terminal region (residues 38–50). The C-terminal region of TTN (residues 41–50 of DBI) is common to all three naturally occurring peptides, ODN (DBI 33–50), EPN (DBI 26–50), and TTN (DBI 17–50).

The predicted helix of TTN has a primary sequence with many characteristics in common with known α-helices. First, the C-terminal amino acid (residue 37) is glycine. This residue is a strong helix terminator, as has been shown by among others Chou and Fasman (11) and more recently by Richardson and Richardson (29).

The N-terminal residue of the predicted helix (Glu_{23}) is negatively charged. As has been pointed out by Chou and Fasman (11) and Richardson and Richardson (29), negative charges tend to be associated statistically with the N-terminal region of the helix. Such negative charges have been proposed

TABLE 2

Relations between α-helix of DBI fragments and ability to displace [^{3}H]flumazenil and [^{3}H]Ro 5-4864 from their binding sites on intact cerebellar granule cells and membrane of cerebellar astrocytes

		α-Helix in MeOH[a]		IC_{50}	
		%	Amino acids	[^{3}H]Flumazenil binding to cerebellar granule cells	[^{3}H]Ro 5-4864 binding to astrocytes membranes
				μM	
TQPTDEEMLFIYSHFKQATVGDVNTDRPGLLDLK	17–50 (TTN)	48	16.3	>100	6
EEMLFIYSHFKQATVGDVNTDRPGLLDLK	22–50	28	7.8	>50	7
FIYSHFKQATVGDVNTDRPGLLDLK	26–50 (EPN)	8	2.2[c]	50	>50
PTDEEMLFIYSHFKQATVGDVNT	19–41	23	5.3	>50	>50
QATVGDVNTDRPGLLDLK	33–50 (ODN)	7	2.0[c]	5	>50
QATVGDVNTDRPGLLDLKNH_2	33–50 (ODNNH_2)			>100	>100

[a] These values were obtained from CD spectra analyses (see Fig. 3 and Table 1). The % helicity and the number of amino acids in the α-helix are determined at 4°C, the same temperature as the binding assay.

[b] The ^{3}H-ligand concentration in the assay mixture was 2 nM (see "Materials and Methods" for details).

[c] The CD spectra of these peptides do not predict α-helical structure (see Fig. 3). The reported values are within the threshold limits.

TABLE 3

Effect of TTN and β-endorphin on [^{3}H]Ro 5-4864 and [^{3}H] dihydroalprenolol binding to rat astrocyte membranes

The ^{3}H-ligand concentration in the assay mixture was 2 nM for [^{3}H]Ro 5-4864 and for [^{3}H]dihydroalprenolol. The dihydroalprenolol binding to the rat astrocyte membranes has an apparent K_D of 2 nM and B_{max} of 110 fmol/mg of protein. Each value is the mean ± standard error of three experiments with five replicates for each experiment.

Peptide	Bound [^{3}H]Ro 5-4864	Bound [^{3}H] dihydroalprenolol
	pmol/mg of protein	*fmol/mg of protein*
None	6.8 ± 0.30	25 ± 1.2
TTN (10 μM)	2.1 ± 0.10[a]	27 ± 2.0
β-Endorphin (10 μM)	7.0 ± 0.25	

[a] $p < 0.01$ when compared with controls.

to stabilize helices either by interacting with the helix macrodipole (30), by formation of hydrogen bonds to unbonded potential amide main chain hydrogen bonds located in the N-terminal region (12), or by a combination of the two. At the predicted N-terminal region there are actually three negative charges, Asp_{21}, Glu_{22}, and Glu_{23}. Although the structural prediction suggests that the N-terminus is Glu_{23}, Richardson and Richardson (29) have pointed out that glutamic acid has a higher probability of occurring at locations 1, 2, and 3 from the actual N-terminal residue. Aspartic acid, on the other hand, has a very high probability of being the N-terminal residue. These observations suggest that the α-helix may extend to Asp_{21}. The first nonhelical residue would then be Thr_{20}. Model building shows that the side chain hydroxyl of Thr_{20} could hydrogen bond to the main chain amide nitrogen of Met_{24}, which would ordinarily be left unbonded at the end of the helix (Fig. 5). This could add increased stability to the helix (12).

Rico *et al.* (31) have proposed that interactions between Phe_8 and the protonated side chain of His_{12} in the ribonuclease S-peptide contribute to the stability of this α-helical region. A similar interaction between the protonated side chain of His_{30} and the side chain of Phe_{26} (or Phe_{31}) may also stabilize the hydrophobic helix in TTN. This is a testable hypothesis. If this interaction is important, the helix stability should titrate with pH and have a transition midpoint of approximately 6.7. There are no other histidines in the peptide.

Interestingly, the residue immediately following the C-terminal glycine (Asp_{38}) is negatively charged. This negative charge may, in fact, partially destabilize the helix by placing a negative charge at the negative pole of the peptide macrodipole. Amino acid substitution at this location would allow this hypothesis to be tested. The two positive charges at the middle of the helix (His_{30} and Lys_{32}) probably have no direct effect on helix stability through interaction with the helix macrodipole. However, as discussed above, His_{30} may stabilize the helix through stacking interactions with Phe_{26} or Phe_{31}.

The results of CD studies certainly support the existence of the α-helix (residues 23–37 in the structure of TTN). Fig. 3A shows that, in MeOH, TTN (DBI 17–50) shows minima at 210 and 220 nm, which are characteristic of an α-helix. Analysis of the spectrum in terms of secondary structure suggests the existence of 16 amino acids, which is in good agreement with the 15 amino acids in the α-helix predicted by the method of Chou and Fasman. This spectrum was measured in 100% MeOH, which is known to stabilize α-helices. The spectrum in water shows virtually no tendency to form an α-helix. As can be seen from Fig. 3B, CD spectra of DBI 22–50 support the existence of an α-helix also in this peptide. However, removal of the five N-terminal residues of TTN has a partial destabilizing effect. Removal of the five-amino acid segment of TTN (residues 17–21) to obtain DBI 22–50 removes Thr_{20} and Asp_{21}. Although this still leaves negative charges at the N-terminus and, therefore, potentially maintains stabilization through interactions with the helix macrodipole, the helix now ends with two glutamic acid residues in a row. As was mentioned above, Richardson and Richardson (29) have shown that glutamic acids are statistically disfavored as helix terminators. Hence, removal of Thr_{20} and Asp_{21} and their stabilizing interactions, as well as the creation of an N-terminal glutamic acid, may be the reason for the destabilization of DBI 22–50 compared with TTN DBI 17–50, even though most of the proposed α-helical residues are still present.

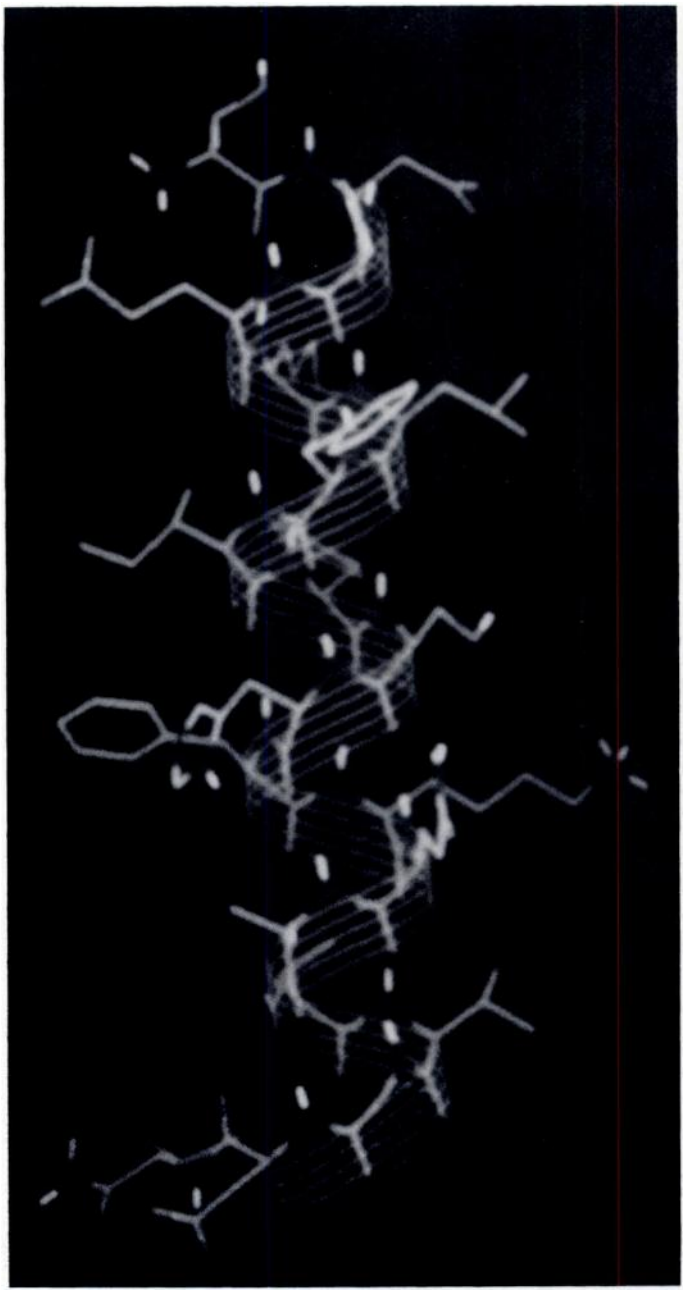

Fig. 5. Computer-generated structure for the proposed α-helix of TTN.

The CD spectrum of EPN (DBI 26–50) shows negligible ellipticity and only two predicted amino acids are in the α-helix. In this peptide, all of the negatively charged N-terminal residues now have been removed and the helical region now ends at Phe_{26}. Richardson and Richardson (29) have shown that phenylalanine is highly disfavored as an N-terminal residue and is more likely to be distributed toward the middle of the α-helix. Chou and Fasman (11) have shown that phenylalanine is only a weak helix-former. Similarly, the potential interaction between the phenyl ring of Phe_{26} and the protonated imidazole ring of His_{30} may also be destabilized when phenylalanine is the N-terminus of the helix. In this position, the side chain is likely to have significantly more conformational mobility.

DBI 19–41 contains the complete predicted hydrophobic helical region as well as four additional N-terminal and four C-terminal residues. This peptide has an average of five amino acids in the helical form. Hence, this helix is significantly destabilized with respect to TTN (DBI 17–50). Because the entire predicted α-helical region is contained in this peptide and, hence, includes all the stabilizing interactions discussed above, it is surprising that this helix shows such dramatically decreased stability. These results suggest that perhaps tertiary interactions from other N-terminal or C-terminal residues in the completely folded state of the peptide may be contributing to helical stability; this hypothesis could be tested using two-dimensional NMR. Finally, ODN (DBI 33–50) is a peptide that contains only the five C-terminal residues predicted to be in the α-helical conformation. All stabilizing interactions have been removed from this α-helix and the destabilizing effect of Asp_{38} remains. Hence, it is not surprising that under all solvent conditions ODN shows virtually no tendency to form an α-helix.

As mentioned above and as discussed by Taylor and Kaiser (25), recognition helices in polypeptide receptor ligands often have an amphipathic nature. However, in Fig. 2, no particular amphipathic character of the α-helix in DBI is obvious. In fact, the hydrophobic amino acids appear to be more or less randomly distributed, in accord with the model of the α-helical part of TTN (Fig. 5). This suggests that the interaction of TTN with its receptor may be qualitatively different for ligands with amphipathic helices.

Erne *et al.* (32) suggest, as a result of IR attenuated total reflection spectroscopy and capacitance minimization, that the tridecapeptide dynorphin 1–13 forms an α-helix when associated with the membrane and that this helix is perpendicularly oriented with respect to the membrane surface. This suggests that a potential aspect of the mechanism by which recognition helices interact with receptors is through membrane insertion. C-terminal α-helix (residues 121–133) in human interleukin-2 is required for full biological activity (33). The fact that the proposed helix in DBI is the most hydrophobic portion of the molecule suggests that this might potentially be true for at least TTN (DBI 17–50). However, in the middle of the helix there are two full positive charges. This argues against the suggestion that the recognition helix in TTN works through insertion into the membrane.

Correlation between structural features and specific BZ binding sites. TTN, the most abundant natural processing product of DBI in rat brain (1, 2), and its structurally related peptides ODN and DBI 22–50 bind selectively to different BZ binding site subtypes. These observations and the information obtained by analyses of CD spectra, hydrophobic characteristics, and amino acid charge distribution support the view that the selection among different BZ binding sites is dictated by the secondary structure of the peptides.

In the central nervous system, BZ binding sites are a heterogeneous population of highly selective recognition molecules. A large number of BZ binding sites are located in neurons at an allosteric modulatory center that is part of the $GABA_A$ receptor (1). These BZ binding sites are part of the GABA receptor domain and are functionally linked to the recognition site for GABA. They have the capacity to mediate positive or negative allosteric modulation on the probability that the primary transmitter GABA opens the anionic channel (34). Molecular cloning (35), molecular electrophysiological studies (36), and ligand binding determination (37) have revealed heterogeneity for the BZ binding sites located on the allosteric modulatory center of $GABA_A$ receptors and have allowed workers to propose the existence of at least two $GABA_A$ receptor subtypes ($GABA_{A1}$ and $GABA_{A2}$) (21). $GABA_{A1}$ and $GABA_{A2}$ receptor subtypes preferentially bind [^{3}H]flumazenil. The existence of a third $GABA_A$ receptor, called the $GABA_{A3}$ receptor subtype, which preferentially binds Ro 5-4864 or PK 11195 but fails to bind flumazenil (21), has been inferred by combined molecular-electrophysiological experiments (38). In addition to BZ binding sites associated with $GABA_A$ receptors, molecular biological and radioreceptor binding studies have revealed the presence of another class of BZ binding site highly concentrated in the membranes of mitochondria isolated from certain peripheral tissues (39–42). In the central nervous system, these mitochondria-linked BZ binding sites are mainly located in glial cells (39).

In the present study, we show that TTN and DBI 22–50 bind with high affinity to BZ binding sites selectively recognized by Ro 5-4864 or PK 11195 but not to BZ binding sites recognized by flumazenil. In contrast, ODN (which contains the same C-terminal region of TTN and DBI 22–50 but lacks the N-terminal region of TTN) prefers BZ binding sites recognized by flumazenil.

DBI 19–41, a peptide that contains only the N-terminal structure of TTN, fails to displace competitively both flumazenil or Ro 5-4864 from the high affinity binding sites associated with $GABA_A$ receptors or mitochondrial receptors. This suggests that the N-terminal region of TTN is not required for recognition at the BZ binding sites. In contrast, the C-terminal region of TTN, which is also present unmodified in DBI 22–50, EPN, and ODN, is essential for the displacement of BZs from their respective binding sites and for the pharmacological proconflict action reported for rats (2, 6). Amidation of the C-terminal lysine in the ODN peptide, as in the case of ODN-NH_2, or removal of the C-terminal region from TTN, as in the case of DBI fragment 19–41, virtually abolishes the isosteric interaction with BZ binding sites (Table 2) and the corresponding pharmacological activity (1, 6).

Hence, the data of Table 2 suggest a correlation between the presence of the predicted α-helical structure in the DBI peptide fragments and their ability to select among the different BZ binding site subtypes. TTN, with a theoretically stable α-helix, has a high affinity for the BZ binding sites recognized by Ro 5-4864 or PK 11195. In contrast, ODN, which shows virtually no tendency to form an α-helix, prefers BZ binding sites selectively

recognized by flumazenil. The importance of the α-helical structure in determining the preference for the different BZ binding subtypes is further stressed by the two peptide analogues of TTN and ODN, DBI 22–50 and EPN (DBI 26–50). These two peptides, whose amino acid sequences are shorter than that of TTN (DBI 17–50) but longer than that of ODN (DBI 33–50), have differences in their α-helical configurations and preferences for BZ binding sites. DBI 22–50 has a theoretically stable α-helix and a high affinity for the Ro 5-4864-preferring BZ binding site. In contrast, EPN lacks a stable α-helix and has low affinity for the Ro 5-4864-preferring BZ binding sites. It also has low affinity for the flumazenil-preferring BZ binding site (see Table 2).

These observations suggest that the principle governing the ability of TTN and ODN to select among recognition site subtypes is guided by the same principle that operates in the selection of opioid recognition site subtypes by opioid peptides and in the selection of tachykinin recognition site subtypes by substance P, neurokinin A, and neurokinin B (25, 28).

It has been postulated that regulatory peptides that do not form tertiary structures have C-terminal or NH_2-terminal regions serving either as "message" or as "address" domains. For example, modeling studies of opioid peptides have indicated that the amino terminal sequence (the message domain) has highly specific interactions with the μ, δ, κ opioid binding sites, and a single amino acid deletion or substitution in this segment reduces or abolishes the biological activity (25, 28). In contrast, the domain of potential α-helix (the carboxyl terminal region of the opioids) acquires address function because it determines the specificity of the message domain for binding to the different opioid receptor subtypes (25, 28). Thus, in analogy with the results with opioid peptide and tachykinins, we propose that the C-terminal TTN, which is also present in the C-terminal region of DBI 22–50, EPN, and ODN, contains the message domain for the different BZ recognition sites. In contrast, the region of potential hydrophobic α-helix at the N-terminal region of TTN or DBI 22–50 assumes an address function, perhaps limiting the receptor-bound conformation of the peptide and ultimately determining the specificity of the message domain for binding to the different BZ recognition subtypes.

Acknowledgement

The assistance of J. Scott-Dixon for the computer-generated structure of Figure 5 is gratefully acknowledged.

References

1. Guidotti, A., H. Alho, A. Berkovich, D. H. Cox, C. Ferrarese, E. Slobodyansky, M. R. Santi, and C. Wambebe. DBI processing: allosteric modulation at different GABA/benzodiazepine receptor subtypes, in *Allosteric Modulation of Amino Acid Receptors: Therapeutic Implications* (E. A. Barnard and E. Costa, eds.). Raven Press, New York, 100–123 (1989).
2. Slobodyansky, E., A. Guidotti, C. Wambebe, A. Berkovich, and E. Costa. Isolation and characterization of a rat brain triakoutatetrancuropeptide, a posttranslational product of diazepam binding inhibitor: specific aeliou at the Ro 5-4846 recognition site. *J. Neurochem.* **53**:1276–1284 (1989).
3. Guidotti, A., C. M. Forchetti, M. G. Corda, D. Konkel, C. D. Bennett, and E. Costa. Isolation, characterization, and purification to homegeneity of an endogenous polypeptide with agonistic action on benzodiazepine receptors. *Proc. Natl. Acad. Sci. USA* **80**:3535–3581 (1983).
4. Gray, P. W., D. Glaister, P. H. Seeburg, A. Guidotti, and E. Costa. Cloning and expression of cDNA for human diazepam binding inhibitor, a natural ligand of an allosteric regulatory site of the *gamma*-aminobutyric acid type A receptor. *Proc. Natl. Acad. Sci. USA* **83**:7547–7551 (1986).
5. Marquardt, H., G. J. Todaro, and M. Shoyab. Complete amino acid sequences of bovine and human endozepines. *J. Biol. Chem.* **261**:9727–9731 (1986).
6. Ferrero, P., M. R. Santi, B. Conti-Tronconi, E. Costa, and A. Guidotti. Study of an octadecaneuropeptide derived from diazepam binding inhibitor (DBI): biological activity and presence in rat brain. *Proc. Natl. Acad. Sci. USA* **83**:827–831 (1986).
7. Merrifield, R. B. Solid phase peptide synthesis. *J. Am. Chem. Soc.* **85**:2149–2154 (1963).
8. Hancock, W. S., and J. E. Battersby. A new micro-test for the detection of incomplete coupling reaction in solid-phase peptide synthesis using 2,4,6-trinitrobenzenesulfonic acid. *Anal. Biochem.* **71**:260–264 (1976).
9. Tam, J. P., W. F. Heath, and R. B. Merrifield. S_n2 deprotection of synthetic peptides with a low concentration of HF in dimethyl sulfide: evidence and application in peptide synthesis. *J. Am. Chem. Soc.* **105**:6442–6455 (1983).
10. Hunkapiller, M. W., and L. Hood. Analyses of phenylthiohydantoins by ultrasensitive gradient high performance liquid chromatography. Methods Enzymol. **91**:486–493 (1983).
11. Chou, P. Y., and G. D. Fasman. Prediction of the secondary structure of proteins from their amino acid sequence. *Adv. Enzymol.* **47**:45–148 (1978).
12. Rose, G. D., L. M. Gierasch, and J. A. Smith. Turns in peptides and proteins. *Adv. Protein Chem.* **37**:1–109 (1985).
13. Kyte, J., and R. F. Doolittle. A simple method for displaying the hydropathic character of a protein. *J. Mol. Biol.* **157**:105–132 (1982).
14. Nozaki, Y., and C. Tanford. The solubility of amino acids and two glycine peptides in aqueous ethanol and dioxane solutions. J. Biol. Chem. **246**:2211–2217 (1971).
15. Hopp, T. P., and K. R. Woods. Prediction of protein antigenic determinants from amino acid sequences. *Proc. Natl. Acad. Sci. USA* **78**:3824–3828 (1981).
16. Provencher, S. W., and J. Glockner. Estimation of globular protein secondary structure from circular dichroism. *Biochemistry* **20**:33–37 (1981).
17. Gallo, V., B. C. Wise, F. M. Vaccarino, and A. Guidotti. *Gamma*-aminobutyric acid benzodiazepine-induced modulation of ^{35}S-*t*-butylbicyclophosphphorotionate binding to cerebellar granule cells. *J. Neurosci.* **5**:2432–2438 (1985).
18. Vaccarino, F. M., H. Alho, M. R. Santi, and A. Guidotti. Coexistence of GABA receptors and GABA-modulin in primary cultures of rat cerebellar granule cells. *J. Neurosci.* **7**:65–76 (1987).
19. Lowry, O. H., N. J. Rosebrough, A. L. Farr, and R. J. Randall. Protein measurement with the Folin phenol reagent. *J. Biol. Chem.* **193**:256–275 (1951).
20. Woodhams, P. L., G. P. Wilkin, and J. Balaz. Rat cerebellar cells in tissue culture II. Immunocytochemical identification of replicating cells in astrocyte-enriched cultures. *Dev. Neurosci.* **4**:307–321 (1981).
21. Barbaccia, M. L., E. Costa, and A. Guidotti. Endogenous ligands for high affinity recognition sites of psychotropic drugs. *Annu. Rev. Pharmacol. Toxicol.* **28**: 451–476 (1988).
22. Bender, A. S., and L. Hertz. Octadecaneuropeptide (ODN: anxiety peptide) displaces diazepam more potently from astrocytic than neuronal binding sites. *Eur. J. Pharmacol.* **13**:335–336 (1986).
23. Costa, E., A. Berkovich, and A. Guidotti. The regulation of GABAergic receptors by a novel family of endogenous neuropeptides. *Life. Sci.* **41**:799–803 (1987).
24. Mohler, H., and J. G. Richards. Distinction of agonists from antagonists: benzodiazepine receptor interaction *in vitro*. *Nature (Lond.)* **294**:763–765 (1981).
25. Taylor, J. N., and E. T. Kaiser. The structural characterization of *beta*-endorphin and related peptide hormones and neurotransmitters. *Pharmacol. Rev.* **38**:291–319 (1986).
26. Penefsky, H. S., Reversible binding of P_i by beef heart mitochondrial adenosine triphosphate *J. Biol. Chem.* **252**: 2891–2899 (1977).
27. Massotti, M., A. Guidotti, and E. Costa. Characterization of benzodiazepine and *gamma*-aminobutyric recognition sites and their endogenous modulators. *J. Neurosci.* **1**:409–418 (1981).
28. Schwyzer, R. Membrane-associated molecular mechanism of neurokinin receptor subtype selection. *EMBO J* **6**:2255–2259 (1987).
29. Richardson, J. S., and D. C. Richardson, Amino acid preferences for specific locations at the end of *alpha*-helices. *Science* (*Wash. D. C.*) **240**:1648–1652 (1988).
30. Shoemaker, K. R., P. S. Kim, E. J. York, J. M. Stewart, and R. L. Baldwin. Test of the helix dipole model for stabilization of *alpha*-helices. *Nature (Lond.)* **326**:563–567 (1987).
31. Rico, M., J. M. Santoro, F. J. Bermejo, J. Hermanz, J. L. Nieto, E. Gallego, and M. A. Jimenez. Thermodynamic parameters for the helix-coil thermal transition of ribonuclease-*S*-peptide and derivatives from ^{1}H-NMR data. *Biopolymers* **25**:1031–1053 (1986).
32. Erne, D., S. F. Sargent. and R. Schwyzer. Preferred conformation, orientation and accummulation of dynorphian A-(1–13)-tridecapeptide on the surface of neutral lipid membranes. *Biochemistry* **24**:4261–4263 (1985).
33. Ju, G., L. Collins, K. L. Kaffker, W. H. Tsien, R. Chizzonite, R. Crow, R. Bhatt, and P. L. Kilian. Structure-function analysis of human interleukin-2. *J. Biol. Chem.* **262**:5723–5731 (1989).
34. Costa, E., H. Alho, M. Favaron, and H. Manev. Pharmacological implications of the allosteric modulation of neurotransmitter amino acid receptors, in *Allosteric Modulation of Amino Acid Receptors: Therapeutic Implications* (E. A. Barnard and E. Costa, eds.). Raven Press, New York, 3–18 (1988).
35. Barnard, E. A., D. R. Burt, M. G. Darlison, N. Fusita, E. S. Levitan, P. R. Schofield, P. H. Seeburg, M. D. Squire, and F. A. Stephenson. Molecular biology of GABA receptor, in in *Allosteric Modulation.of Amino Acid Recep-*

tors: Therapeutic Implications (E. A. Barnard and E. Costa, eds). Raven Press, New York, 19–30 (1989).
36. Levitan, E. S., P. R. Schofield, D. R. Burt, L. M. Rhee, W. Wisden, M. Kohler, N. Fujita, H. F. Rodriguez, A. Stephenson, M. G. Darlison, E. A. Barnard and P. M. Seeburg. Structural and functional basis for $GABA_A$ receptor heterogeneity. *Nature (Lond.)* **335**:76–79 (1988).
37. Santi, M. R., D. H. Cox, and A. Guidotti. Heterogeneity of GABA/benzodiazepine/*beta*-carboline receptor complex in rat spinal cord. J. Neurochem. **50**: 1080–1086 (1988).
38. Puia, G., M. R. Santi, S. Vicini, D. B. Pritchett, P. H. Seeburg, and E. Costa. Differences in the negative allosteric modulation of *gamma*-aminobutyric $acid_A$ receptors elicited by 4′-chlorodiazepam and by a *beta*-carboline 3-carboxylate ester: a study with natural and reconstituted receptors. *Proc. Natl. Acad. Sci. USA*, **86**:7275–7279 (1989).
39. Anholt, R. R. H. Mitochondrial benzodiazepine receptors as potential modulators of intermediary metabolism. *Trends Pharmacol. Sci.* 506–511 (1986).
40. Antkiewicz-Michaluk, L., A. Guidotti, K. E. Krueger. Molecular characterization and mitochondrial density of a recognition site for peripheral-type benzodiazepine ligands. *Mol. Pharmacol.* **34**:272–278 (1988).
41. Antkiewicz-Michaluk, L., A. G. Mukhin, A. Guidotti, and K. E. Krueger. Purification and characterization of a protein associated with peripheral-type benzodiazepine binding sites. *J. Biol. Sci.* **263**:17317–17321 (1988).
42. Sprengel, R., P. Werner, P. H. Seeburg, A. G. Mukhin, M. R. Santi, D. R. Grayson, A. Guidotti, and K. E. Krueger. Molecular cloning and expression of cDNA encoding a peripheral-type benzodiazepine receptor. *J. Biol. Chem.*, **266**:20415–20421 (1989).

Send reprint requests to: Alessandro Guidotti, Fidia-Georgetown Institute for the Neurosciences, 3900 Reservoir Road, N.W., Washington, DC 20007.